AIAA SciTech Forum
8-12 January 2024, Orlando, FL
AIAA SCITECH 2024 Forum

10.2514/6.2024-2689

Tail-Assisted Pitch Control in Flying Lizards

Shane D. Ross*, Mohamed Zakaria†, and John J. Socha‡
Virginia Tech, Blacksburg, VA, 24061, USA

Tyson L. Hedrick§
University of North Carolina at Chapel Hill, Chapel Hill, NC 27599, USA

Pranav C. Khandelwal¶
Max Planck Institute for Intelligent Systems, 70569 Stuttgart, Germany

Arboreal animals face challenges in maneuvering through complex terrain, and directed aerial descent or gliding flight offers a solution despite control difficulties. While some animals possess specialized structures for aerodynamic control, many arboreal species may rely on tail-assisted attitude control in mid-air. This study examines the role of tail inertial and aerodynamic forces in mid-air reorientation behaviors based on field experiment data from *Draco* "flying" lizards along with mathematical models. Modeling results suggest that the tail, which represents only about 5% of the lizard's mass and surface area, plays a significant role in pitch control in flying lizards. Furthermore, the aerodynamic effect of the tail is found to be significant, particularly in concert with the inertial effect.

I. Introduction

Gliding, as a unique type of locomotion, can be defined by horizontal non-thrust generating movement [1–3]. Almost all gliding species exhibit anatomical alterations which enable them to generate and manipulate aerodynamic forces, facilitating descent while traveling through the air. Examples include gliding ants, snakes, flying lizards, and flying squirrels [2, 4–7]. Gliding is also part of a propulsion technique known as fluke-and-glide [8] seen in some aquatic species. This method involves the oscillatory motion of the tail fin to move through water, followed by a period where the animal glides with a fixed posture. Such a strategy is key to the efficient employment of energy in these creatures, allowing them to conserve energy while swimming. This technique is especially prevalent in species like seals, sharks, and dolphins, who use it to balance energy expenditure with effective locomotion [9–12].

Non-flapping flyers are not the only ones that make use of gliding. Birds, insects, and bats make use of gliding in variety of ways [13–15]. For instance, albatrosses use the process of dynamic soaring (the use of wind shear to generate lift) to enable them to travel large distances in a sustained energy efficient non-flapping flight [16–18]. Another study concerning flapping flyers showed that barn owls (*Tyto alba*) use their tails in gliding to reduce overall drag by pointing it downwards [19]. This also tells us that the tail affects the glide dynamics.

Mammalian gliders, flying lizards (*Draco dussumieri*), and flying snakes (*Chrysopelea paradisi*) exhibit tail movements during some or all components of the glide [2, 20]. As a long appendage, the tail may provide both inertial and aerodynamic functions that influence the glide. Tails essentially consist of a flexible vertebral column surrounded by muscle, providing the capability for active control. However, as a long thin appendage, the tail is also subject to passive fluid-structure interactions, and so it is unclear how tail kinematics reflect active versus passive effects for these gliders [1]. From video recordings, the tails of flying snakes give the appearance of passive and somewhat haphazard movements that result from the body's undulation [21, 22], but *Draco* flying lizards appear to exhibit more deliberate control, as discussed below.

The tail could be used for controlling movements during all three major components of the glide: takeoff, gliding, and landing (see Fig. 1(b)). In *Draco* flying lizards, rapid tail movement can be seen during takeoff while the animal reorients, such that its ventral side (underside) faces the ground. This reorientation is likely causally linked to the tail. Previous work on the gliding gecko *Hemidactylus platyurus* demonstrated the use of tail as an *inertial* appendage for

*Professor, Kevin T. Crofton Department of Aerospace and Ocean Engineering, Virginia tech.
†PhD Student, Kevin T. Crofton Department of Aerospace and Ocean Engineering, Virginia Tech, AIAA Student Member.
‡Professor, Department of Biomedical Engineering and Mechanics, Virginia Tech.
§Professor, Department of Biology, University of North Carolina at Chapel Hill.
¶Senior Postdoctoral Researcher, Max Planck Institute for Intelligent Systems.

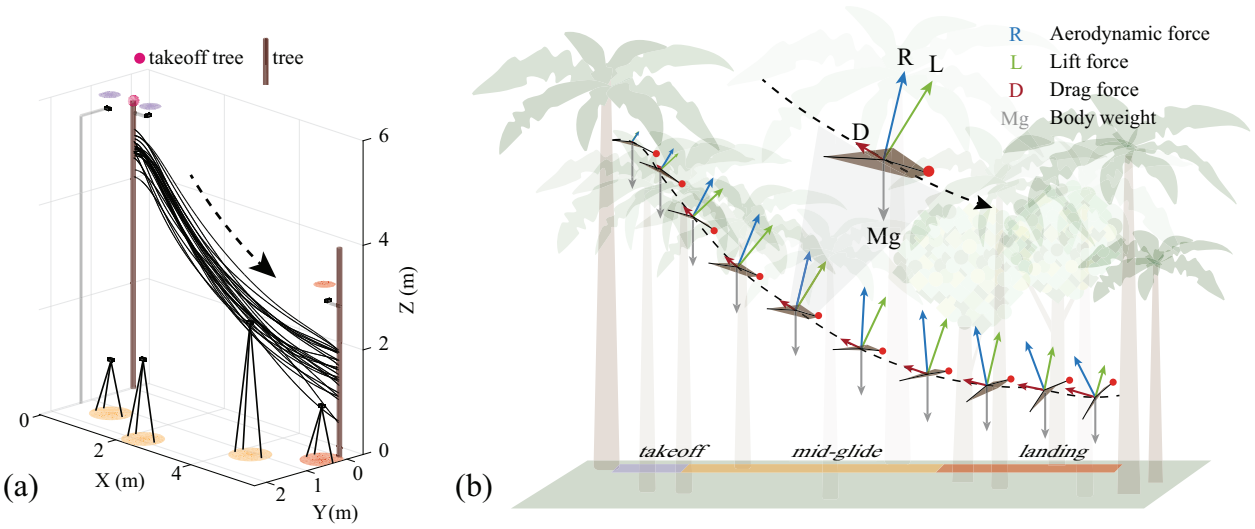

Fig. 1 (a) A scaled illustration of the motion capture arena showing all 24 smoothed glides and the seven camera positions used to collect 3D kinematic data. The seven cameras are divided into three groups (color coded) based on the part of the glide they record. The takeoff cameras are marked by purple discs, mid-glide cameras with orange, and landing cameras with red. (b) Free body diagram showing the forces experienced by a gliding animal's *body* at various stages of the complete glide as well as the change in body orientation. The glide is further divided into the three distinct glide phases of takeoff, mid-glide, and landing. Modified with permission from Khandelwal and Hedrick [27].

reorientation while falling [23, 24]. *H. platyurus* rotates its tail during the fall and, taking advantage of the conservation of angular momentum, reorients itself from ventral side up to the ventral side facing the direction of the fall.

Body reorientation may be a common feature of all gliders, part of an aerial righting reflex that adjusts the posture of the animal to one in which the dorsal side is uppermost and is advantageous for gliding or preventing injury during a fall [25]. During a glide, small tail movements could be used to effect changes in roll, pitch, or yaw; however, their use to control stability or the direction of the glide trajectory remains largely unexplored. During the landing phase, the tail of the *Draco* flying lizard is positioned closer to the dorsal side of the body, which might facilitate a 'pitch up' motion, attaining an upright body pose to land on a vertical surface such that the forelimbs make contact with the tree first. Recently, it has also been hypothesized that the tail might be used to modulate the center of mass with respect to the center of aerodynamic pressure to initiate pitch control in gliding animals [26]. In simulations that modulated tail position to maintain a fixed angle of attack, the *Draco* flying lizard glided nearly twice as far than without tail control.

In this study, we develop a mathematical model to determine the role of the tail in *Draco* glides. We expanded upon the research conducted by Khandelwal and Hedrick [27], in which they documented voluntary gliding maneuvers executed by a group of wild gliding *Draco* lizards. This investigation took place within a motion capture arena equipped with seven cameras, strategically positioned in the lizards' natural habitat (Fig. 1(a)). The field site was an abandoned areca nut plantation located within the Agumbe Rainforest Research Station campus, Karnataka, India and previously described in [28].

II. Methodology

A. Motion capture data

As described in [27], a field study was conducted at an abandoned areca nut plantation within the Agumbe Rainforest Research Station campus, Karnataka, India from February to April 2017, during which 33 unique individuals (16 males and 17 females) inhabiting the plantation were identified. Glide data from these individuals were collected by constructing a motion capture arena on an approximately 6 m × 7 m patch of the plantation containing two areca nut trees 5.50 m apart with no trees in between. The two trees were designated as the takeoff and landing tree for glide recordings. An array of seven GoPro Hero4 Black cameras (GoPro, Inc) in wide field of view mode were used

together to record the complete lizard glide from various viewing angles between the takeoff and landing tree (Fig. 1(a)). Individual lizard mass and morphology was taken post-glide.

3D position data, (X, Y, Z) inertial coordinates, were obtained using the MATLAB (The MathWorks, Natick, MA, USA) package DLTdv8. For each glide recording, seven body points on the dorsal side of the lizard in each frame of the complete glide were digitized: five on the body and two on the tail (Fig. 2(a)). The five body points corresponded to locations on the anterior, middle, and posterior part of the lizard's body, and the left- and right-wing tip. The two tail points corresponded to the mid-tail and tail-end. Each point was digitized in all camera views in which it was visible (at least in two or more camera views per frame throughout the complete glide). These resulted in seven tracks representing the complete glide trajectory with no missing digitization data. The mid-body point was used as a proxy for the center of mass and whole glide kinematic calculations including velocity and acceleration. Thereafter, each glide was divided into the takeoff, mid-glide, and landing phase (Fig. 1(a)) based on previously established criteria in [28].

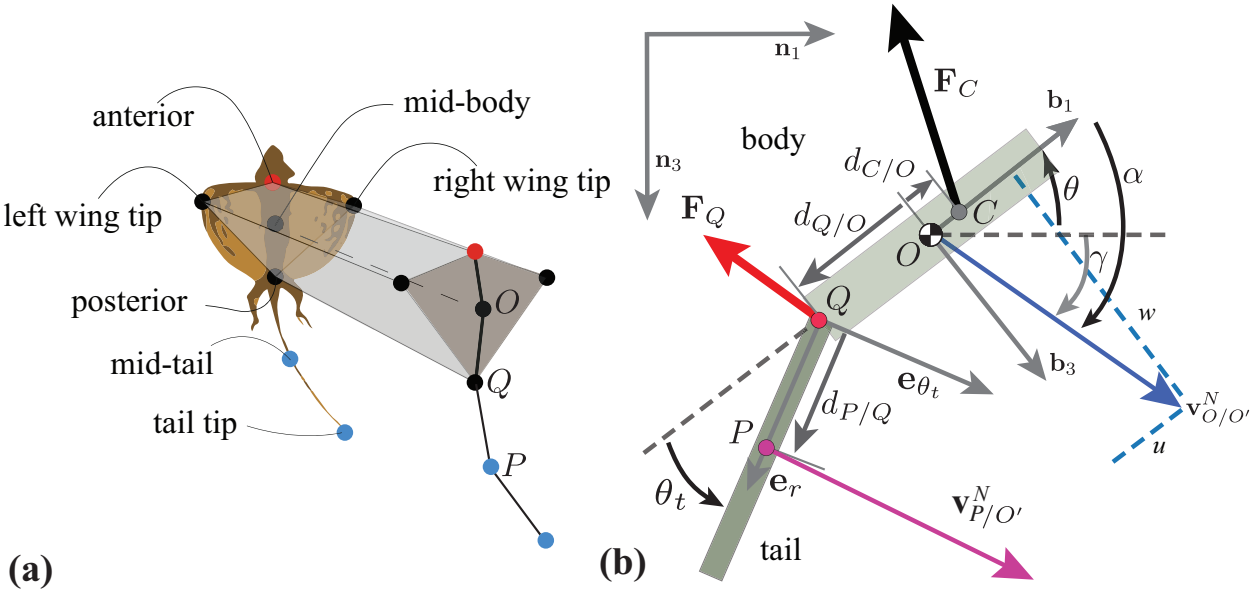

Fig. 2 (a) Illustration showing the seven points tracked per frame for each glide. Modified with permission from Khandelwal and Hedrick [27]. (b) Schematic of *Draco* lizard body-tail system in 2D showing a positive angle-of-attack α, positive pitch θ, positive glide angle γ, and positive tail angle θ_t.

B. Mathematical model of longitudinal dynamics

In this study, we focus only on the longitudinal dynamics—i.e., dynamics in the XZ plane.

1. Dynamics of the 2D system

From the motion capture data, We are originally given the velocity components compared to an inertial frame oriented like $\{\mathbf{n}_1, \mathbf{n}_3\}$ in Fig. 2(b). That is, we are given,

$$\mathbf{v}^N_{O/O'} = v_x \mathbf{n}_1 - v_z \mathbf{n}_3 \tag{1}$$

and must transform to the body-fixed $\{\mathbf{b}_1, \mathbf{b}_3\}$ directions via,

$$\begin{aligned} u &= v_x \cos\theta + v_z \sin\theta \\ w &= v_x \sin\theta - v_z \cos\theta. \end{aligned} \tag{2}$$

2. Dynamics of the body

For the longitudinal motion of the body of mass, m_b, Newton's 2nd law gives,

$$m_b \mathbf{a}^N_{O/O'} = \mathbf{F}_{\text{total}}, \tag{3}$$

where the total force on the body is,

$$\mathbf{F}_{\text{total}} = \mathbf{F}_{\text{grav}} + \mathbf{F}_{\text{aero}} - \mathbf{F}_Q, \tag{4}$$

where the first term is gravity, $\mathbf{F}_{\text{grav}} = m_b g \mathbf{n}_3$, where $\mathbf{n}_3 = -\sin\theta \mathbf{b}_1 + \cos\theta \mathbf{b}_3$, the second is the aerodynamic force due to the body airfoil, $\mathbf{F}_{\text{aero}} = F_x \mathbf{b}_1 + F_z \mathbf{b}_3$, and the reaction force due to the tail is $-\mathbf{F}_Q = \left(F_{\text{iner,t}_x} + F_{\text{aero,t}_x}\right) \mathbf{b}_1 + \left(F_{\text{iner,t}_z} + F_{\text{aero,t}_z}\right) \mathbf{b}_3$. Note, the minus sign in front of $\mathbf{F}_Q$ is because this must be opposite the force on the tail. So re-writing eq. (3), we get,

$$\begin{aligned}
\dot{u} &= \left(F_x + F_{\text{inert,t}_x} + F_{\text{aero,t}_x} - m_b g \sin\theta\right)/m_b - qw \\
\dot{w} &= \left(F_z + F_{\text{iner,t}_z} + F_{\text{aero,t}_z} + m_b g \cos\theta\right)/m_b + qu \\
\dot{q} &= \left(M_{\text{aero,b}} + M_{\text{iner}_t} + M_{\text{aero}_t}\right)/I_y \\
\dot{\theta} &= q
\end{aligned} \tag{5}$$

where F_x and F_z are the aerodynamic forces due to the body and I_y is the pitch moment of inertia. Instantaneous coefficients of lift and drag, C_L and C_D, were calculated from the kinematic experimental data, ignoring the tail, as described in [27].

In simulation, we have the drag and lift directions, $\{\mathbf{d}_D, \mathbf{d}_L\}$, related to the body-fixed $\{\mathbf{b}_1, \mathbf{b}_3\}$ directions,

$$\begin{bmatrix} \mathbf{b}_1 \\ \mathbf{b}_3 \end{bmatrix} = \begin{bmatrix} -\cos\alpha & \sin\alpha \\ -\sin\alpha & -\cos\alpha \end{bmatrix} \begin{bmatrix} \mathbf{d}_D \\ \mathbf{d}_L \end{bmatrix} \tag{6}$$

So the force coefficients in the $\mathbf{b}_1$ and $\mathbf{b}_3$ directions, respectively, are,

$$\begin{aligned}
C_x &= -C_D(\alpha)\cos\alpha + C_L(\alpha)\sin\alpha \\
C_z &= -C_D(\alpha)\sin\alpha - C_L(\alpha)\cos\alpha
\end{aligned} \tag{7}$$

Where C_x and C_z are the forces transformed into the body frame of the lizard, and the angle of attack,

$$\alpha = \tan^{-1}\left(\frac{w}{u}\right) \tag{8}$$

where $\alpha = \gamma + \theta$, with θ the body pitch angle and γ the glide angle, as oriented in Fig. 2(b).

Finally we have,

$$\begin{aligned}
F_x &= QSC_x \\
F_z &= QSC_z
\end{aligned} \tag{9}$$

where Q is the dynamic pressure term and equals $Q = \frac{1}{2}\rho||\mathbf{v}^N_{O/O'}||^2$, S is the body wing area, and $||\mathbf{v}^N_{O/O'}||^2 = u^2 + w^2$.

3. Dynamics of the tail

The equation of translational motion of the tail is,

$$m_t \mathbf{a}^N_{P/O'} = \mathbf{F}_{gt} + \mathbf{F}_{Dt} + \mathbf{F}_Q, \tag{10}$$

where we will seek an expression for $\mathbf{F}_Q$ to plug into the body dynamic equation, eq. (4) The transformation between the tail-fixed $[\mathbf{e}_r, \mathbf{e}_{\theta_t}\}$ and the body-fixed $\{\mathbf{b}_1, \mathbf{b}_3\}$ directions is,

$$\begin{bmatrix} \mathbf{e}_r \\ \mathbf{e}_{\theta_t} \end{bmatrix} = \begin{bmatrix} -\cos\theta_t & \sin\theta_t \\ \sin\theta_t & \cos\theta_t \end{bmatrix} \begin{bmatrix} \mathbf{b}_1 \\ \mathbf{b}_3 \end{bmatrix} \tag{11}$$

The inertial velocity of the tail in 2D is as follows, in the B-frame,

$$\mathbf{v}^N_{P/O'} = \begin{bmatrix} u + L_t \sin\theta_t(\dot{\theta} + \dot{\theta}_t) \\ w + L_t \cos\theta_t(\dot{\theta} + \dot{\theta}_t) + x_{Q/O}\dot{\theta} \end{bmatrix}_B, \tag{12}$$

where L_t is the length of the tail.

The transverse velocity of the tail (that is, in the $\mathbf{e}_{\theta_t}$ direction), is $v_{t\perp} = \mathbf{v}^N_{P/O'} \cdot \mathbf{e}_{\theta_t}$,

$$v_{t\perp} = \left(u + L_t \sin\theta_t(\dot{\theta} + \dot{\theta}_t)\right)\sin\theta_t + \left(w + L_t \cos\theta_t(\dot{\theta} + \dot{\theta}_t) + x_{Q/O}\dot{\theta}\right)\cos\theta_t \tag{13}$$

If $v_{t\perp} > 0$, then the tail drag force is in the $-\mathbf{e}_{\theta_t}$ direction, and if $v_{t\perp} < 0$, then the tail drag force is in the $\mathbf{e}_{\theta_t}$ direction.

$$\mathbf{F}_{Dt} = \begin{cases} -Q_t S_t C_t \mathbf{e}_{\theta_t} & \text{for } v_{t\perp} > 0 \\ Q_t S_t C_t \mathbf{e}_{\theta_t} & \text{for } v_{t\perp} < 0 \end{cases} \tag{14}$$

where,

$$Q_t = \tfrac{1}{2}\rho v_{t\perp}^2 \tag{15}$$

S_t is the area of the tail, C_t is the coefficient of drag, and

$$\mathbf{e}_{\theta_t} = \begin{bmatrix} \sin\theta_t \\ \cos\theta_t \end{bmatrix}_B . \tag{16}$$

Now, $-\mathbf{F}_Q$, which can be decomposed into $\mathbf{F}_{\text{iner,t}}$ and $\mathbf{F}_{\text{aero,t}}$ is given by,

$$-\mathbf{F}_Q = \mathbf{F}_{gt} + \mathbf{F}_{Dt} - m_t \mathbf{a}^N_{P/O'}, \tag{17}$$

If we take the tail angle $\theta_t(t)$ as an input as a function of time, and initial conditions $(u(0), w(0), q(0), \theta(0))$, we can solve for the body dynamics via eq. (4).

III. Results

We compared body kinematics (u, w, q, θ) from the experimental data for the mid-glide phase only, for four cases: no tail, tail with only inertial effects, tail with only aerodynamic effects, and full tail (inertial andaerodynamic effects). Results for a typical glide trial are shown in Fig. 3. One of the first things to notice is the huge effect the tail has on the pitch rate q. As can be seen in Fig 3, in the presence of no tail forces, the pitch rate q is constantly increasing, causing the pitch θ to overshoot. The absence of tail forces seems to significantly affect the *Draco* lizard's stability and control. The continuous increase in pitch rate q suggests a lack of damping or control authority that might typically be provided by the tail. An additional question that might be of interest is the question of the threshold: Is there a point where θ becomes uncontrollable? This is a question that is still under investigation.

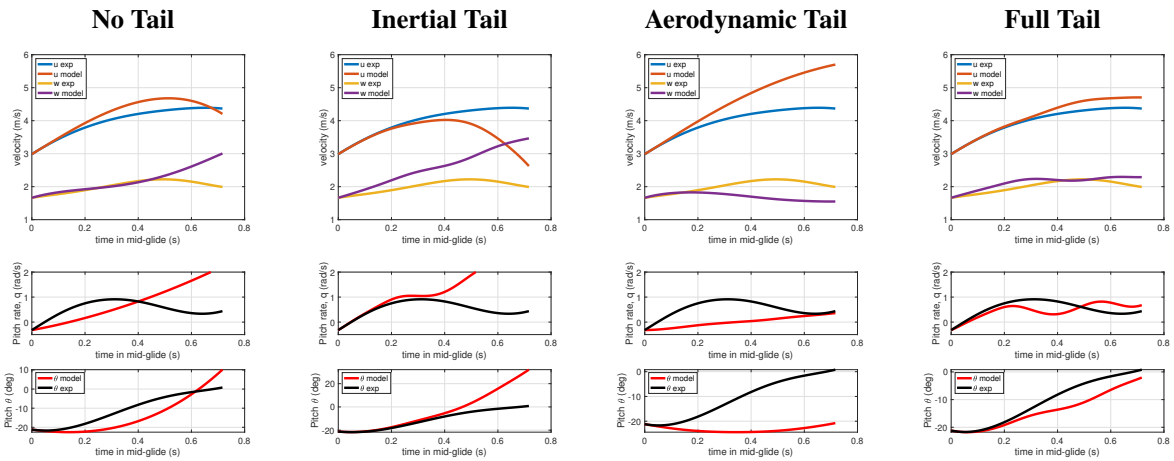

Fig. 3 Body velocities (u, w), pitch θ and pitch rate q with time. In the upper plots, the blue and yellow curves are the experimental u and w body velocities, respectively. In the middle and lower plots, the black curve is the experimental data. The kinematics, pitch θ and pitch rate q are displayed for three cases going from left to right: no tail forces considered, only inertial tail forces only considered, only aerodynamic tail forces considered, and full tail forces (both inertial and aerodynamic forces considered).

The presence of inertial tail forces, even without aerodynamic forces, seems to have a stabilizing effect compared to the scenario with no tail forces. This suggests that inertia plays a significant role in damping the pitch rate. The slope of the pitch rate q curve in the inertial tail force scenario might be less steep than in the no tail force case, indicating a slower rate of destabilization. The addition of aerodynamic tail forces appears to provide further stabilization. This can be seen if the pitch rate q and pitch θ are more controlled and exhibit less overshoot compared to the inertial only scenario. The role of aerodynamic forces in fine-tuning the control and response of the *Draco* lizard is seen to be significant especially when comparing inertial only and the no tail cases.

Regarding the velocities in Fig. 3, and with both inertial and aerodynamic tail forces present, there's likely a more pronounced stabilizing effect on both the x and z body velocities. This results in smoother velocity profiles, reflecting a more controlled and stable flight dynamic, as seen in the pitch rate and angle stabilization. One of the trends that can be seen when comparing the inertial only case and the full tail case is the tuning and the damping effect of the tail aerodynamic forces. The aerodynamic tail forces act like an elevator of an aircraft in the sense that without it, the *Draco* lizard final pitch angle θ overshoots. Also, the x body velocity u greatly decreases without the tail aerodynamic forces. One can visualize that better using Fig 2, as the tail drag force is pointing in the opposite direction of $\boldsymbol{V}_P^N/O'$. This force causes the body to pitch down, and thereby, for a constant flight path angle, the angle of attack to decrease too. In the absence of this force, the increase in the angle of attack will cause an increase in the drag, which can thereby decrease the magnitude of the body velocity u.

Fig 4 further supports our prediction in the importance of the tail aerodynamic forces. As can be seen, the absence of the aerodynamic tail forces causes the RMS error of the pitch rate q to increase. The presence of the inertial forces alone caused the *Draco* to be even more unstable than having no tail, which tells us that the tail aerodynamic forces act in opposition to the tail inertial forces to produced the optimal needed force for the glide.

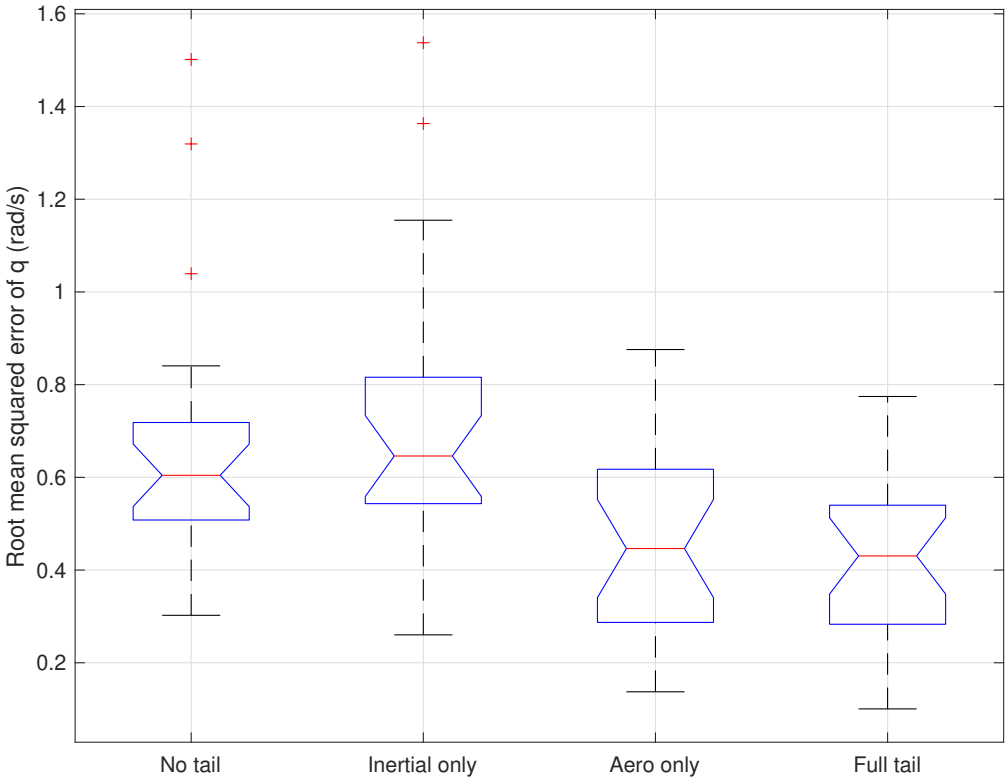

Fig. 4 Mean RMS error of q for each trial during mid-glide for the four model situations, no tail, inertial tail only, aero tail only, and full tail effects (inertial + aerodynamic).

IV. Conclusion

The mathematical model shows the importance of both the aerodynamic and inertial effects of the tail on the overall gliding behavior during mid-glide for *Draco* flying lizards. While the significance of the inertial tail effect was known in the context of jumping lizards [29], the importance of the aerodynamic tail effect was not previously known. As the air speeds involved in gliding are significantly larger than the speeds involved in jumping, this is perhaps not surprising. But to the authors' knowledge, this is the first time the tail aerodynamic effect has been shown to be an important component of flight control in gliding.

Acknowledgments

This work was partially supported by the National Science Foundation under grant 2027523 to S. D. Ross & J. J. Socha.

References

[1] Khandelwal, P. C., Ross, S. D., Dong, H., and Socha, J. J., "Convergence in Gliding Animals: Morphology, Behavior, and Mechanics," *Convergent Evolution: Animal Form and Function*, Springer, 2023, Chap. 13, pp. 391–429.

[2] Socha, J. J., Jafari, F., Munk, Y., and Byrnes, G., "How animals glide: from trajectory to morphology," *Canadian Journal of Zoology*, Vol. 93, No. 12, 2015, pp. 901–924.

[3] Dudley, R., Byrnes, G., Yanoviak, S. P., Borrell, B., Brown, R. M., and McGuire, J. A., "Gliding and the functional origins of flight: biomechanical novelty or necessity?" *Annu. Rev. Ecol. Evol. Syst.*, Vol. 38, 2007, pp. 179–201.

[4] Thorington Jr, R. W., Darrow, K., and Anderson, C. G., "Wing tip anatomy and aerodynamics in flying squirrels," *Journal of Mammalogy*, Vol. 79, No. 1, 1998, pp. 245–250.

[5] Bishop, K. L., "The relationship between 3-D kinematics and gliding performance in the southern flying squirrel, Glaucomys volans," *Journal of Experimental Biology*, Vol. 209, No. 4, 2006, pp. 689–701.

[6] Bahlman, J. W., Swartz, S. M., Riskin, D. K., and Breuer, K. S., "Glide performance and aerodynamics of non-equilibrium glides in northern flying squirrels (Glaucomys sabrinus)," *Journal of The Royal Society Interface*, Vol. 10, No. 80, 2013, p. 20120794.

[7] Yanoviak, S. P., Munk, Y., Kaspari, M., and Dudley, R., "Aerial manoeuvrability in wingless gliding ants (Cephalotes atratus)," *Proceedings of the Royal Society B: Biological Sciences*, Vol. 277, No. 1691, 2010, pp. 2199–2204.

[8] Zhang, D., Wang, Y., Gabaldon, J., Lauderdale, L. K., Miller, L. J., Barton, K., and Shorter, K. A., "Dynamics and Energetics of Bottlenose Dolphin (*Tursiops truncatus*) Fluke-and-Glide Gait," *Journal of Experimental Biology*, 2023, pp. jeb–245237.

[9] Williams, T. M., "Intermittent swimming by mammals: a strategy for increasing energetic efficiency during diving," *American Zoologist*, Vol. 41, No. 2, 2001, pp. 166–176.

[10] Floryan, D., Van Buren, T., and Smits, A. J., "Forces and energetics of intermittent swimming," *Acta Mechanica Sinica*, Vol. 33, 2017, pp. 725–732.

[11] Kramer, D. L., and McLaughlin, R. L., "The behavioral ecology of intermittent locomotion," *American Zoologist*, Vol. 41, No. 2, 2001, pp. 137–153.

[12] Xia, D., Chen, W.-s., Liu, J.-k., and Luo, X., "The energy-saving advantages of burst-and-glide mode for thunniform swimming," *Journal of Hydrodynamics*, Vol. 30, 2018, pp. 1072–1082.

[13] Bomphrey, R. J., Nakata, T., Henningsson, P., and Lin, H.-T., "Flight of the dragonflies and damselflies," *Philosophical Transactions of the Royal Society B: Biological Sciences*, Vol. 371, No. 1704, 2016, p. 20150389.

[14] Thomas, A. L., Jones, G., Rayner, J. M., and Hughes, P. M., "Intermittent gliding flight in the pipistrelle bat (Pipistrellus pipistrellus)(Chiroptera: Vespertilionidae)," *Journal of Experimental Biology*, Vol. 149, No. 1, 1990, pp. 407–416.

[15] Tobalske, B. W., "Morphology, velocity, and intermittent flight in birds," *American Zoologist*, Vol. 41, No. 2, 2001, pp. 177–187.

[16] Denny, M., "Dynamic soaring: aerodynamics for albatrosses," *European Journal of Physics*, Vol. 30, No. 1, 2008, p. 75.

[17] Sachs, G., "Minimum shear wind strength required for dynamic soaring of albatrosses," *Ibis*, Vol. 147, No. 1, 2005, pp. 1–10.

[18] Sachs, G., Traugott, J., Nesterova, A., and Bonadonna, F., "Experimental verification of dynamic soaring in albatrosses," *Journal of Experimental Biology*, Vol. 216, No. 22, 2013, pp. 4222–4232.

[19] Song, J., Cheney, J. A., Bomphrey, R. J., and Usherwood, J. R., "Virtual manipulation of tail postures of a gliding barn owl (Tyto alba) demonstrates drag minimization when gliding," *Journal of the Royal Society Interface*, Vol. 19, No. 187, 2022, p. 20210710.

[20] Khandelwal, P., Shankar, C., and Hedrick, T., "Take-off biomechanics in gliding lizards," *Integrative and Comparative Biology*, Vol. 58, Oxford University Press, 2018, pp. E116–E116.

[21] Socha, J. J., Miklasz, K., Jafari, F., and Vlachos, P. P., "Non-equilibrium trajectory dynamics and the kinematics of gliding in a flying snake," *Bioinspiration & Biomimetics*, Vol. 5, No. 4, 2010, p. 045002.

[22] Yeaton, I. J., Ross, S. D., Baumgardner, G. A., and Socha, J. J., "Undulation enables gliding in flying snakes," *Nature Physics*, Vol. 16, No. 9, 2020, pp. 974–982.

[23] Jusufi, A., Goldman, D. I., Revzen, S., and Full, R. J., "Active tails enhance arboreal acrobatics in geckos," *Proceedings of the National Academy of Sciences*, Vol. 105, No. 11, 2008, pp. 4215–4219.

[24] Jusufi, A., Kawano, D. T., Libby, T., and Full, R. J., "Righting and turning in mid-air using appendage inertia: reptile tails, analytical models and bio-inspired robots," *Bioinspiration & Biomimetics*, Vol. 5, No. 4, 2010, p. 045001.

[25] Jusufi, A., Zeng, Y., Full, R. J., and Dudley, R., "Aerial righting reflexes in flightless animals," *Integrative and Comparative Biology*, Vol. 51, No. 6, 2011, pp. 937–943.

[26] Clark, J., Clark, C., and Higham, T. E., "Tail Control Enhances Gliding in Arboreal Lizards: An Integrative Study Using a 3D Geometric Model and Numerical Simulation: Complimentary/Contributed Paper," *Integrative and Comparative Biology*, Vol. 61, No. 2, 2021, pp. 579–588.

[27] Khandelwal, P. C., and Hedrick, T. L., "Combined effects of body posture and three-dimensional wing shape enable efficient gliding in flying lizards," *Scientific Reports*, Vol. 12, No. 1, 2022, p. 1793.

[28] Khandelwal, P. C., and Hedrick, T. L., "How biomechanics, path planning and sensing enable gliding flight in a natural environment," *Proceedings of the Royal Society B*, Vol. 287, No. 1921, 2020, p. 20192888.

[29] Libby, T., Moore, T. Y., Chang-Siu, E., Li, D., Cohen, D. J., Jusufi, A., and Full, R. J., "Tail-assisted pitch control in lizards, robots and dinosaurs," *Nature*, Vol. 481, No. 7380, 2012, p. 181.